PHYSICAL REVIEW B **77**, 195430 (2008)

Theory of anomalous quantum Hall effects in graphene

P. M. Ostrovsky,[1,2] I. V. Gornyi,[1,*] and A. D. Mirlin[1,3,†]
[1]*Institut für Nanotechnologie, Forschungszentrum Karlsruhe, 76021 Karlsruhe, Germany*
[2]*L. D. Landau Institute for Theoretical Physics RAS, 119334 Moscow, Russia*
[3]*Institut für Theorie der kondensierten Materie, Universität Karlsruhe, 76128 Karlsruhe, Germany*
(Received 14 January 2008; revised manuscript received 27 March 2008; published 22 May 2008)

We develop a theory of anomalous quantum Hall effects in graphene. We demonstrate that the Landau level structure by itself is not sufficient to determine the form of the quantum Hall effect. It is only a special symmetry of disorder that gives rise to anomalous quantization of Hall conductivity in graphene. We analyze the symmetries of disordered single- and double-layer graphene samples in magnetic field and identify the conditions for anomalous Hall quantization.

DOI: 10.1103/PhysRevB.77.195430 PACS number(s): 73.23.−b, 73.43.−f, 73.22.−f

I. INTRODUCTION

Recent successes in manufacturing of atomically thin graphite samples[1] (graphene) have stimulated intense experimental and theoretical activity.[2,3] The key feature of graphene is the massless Dirac type of low-energy electron excitations. This gives rise to a number of unusual physical properties of this system distinguishing it from conventional two-dimensional (2D) metals. One of the most remarkable properties of graphene is the anomalous quantum Hall effect.[4–8] It is extremely sensitive to the structure of the system; in particular, it clearly distinguishes single- and double-layer samples. In spite of the impressive experimental progress, the theory of quantum Hall effect in graphene has not been established. This theory is a subject of the present paper.

As discovered[9] in 1980, the Hall conductivity σ_{xy} of a 2D electron gas in a strong transverse magnetic field develops plateaus at values quantized in units of e^2/h. This phenomenon is the famous integer quantum Hall effect[10] (QHE)—one of the most fascinating quantum effects in the condensed matter physics.

The experimentally measured Hall conductivity of single-layer graphene[4,5,7] is quantized taking the odd multiples of the quantum $2e^2/h$ (here, the factor of 2 is due to the spin degeneracy),

$$\sigma_{xy} = (2k+1)2e^2/h, \quad k \in \mathbb{Z}. \tag{1}$$

In double-layer samples, the quantum Hall plateaus occur at even multiples of $2e^2/h$ excluding $k=0$. Due to this unusual quantization, the Hall measurements are widely used in modern experiments for characterizing the graphene samples. Remarkably, the signatures of Hall conductivity quantization in graphene were recently observed even at room temperature.[7]

A simple argument in favor of the odd QHE [Eq. (1)] in a single graphene layer[11] is based on the structure of Landau levels for two-dimensional massless electrons.[12] In clean graphene, the energies of Landau levels are $\epsilon_N = \hbar\omega_c \operatorname{sgn} N\sqrt{|N|}$ with $\omega_c = v_0\sqrt{2eB/\hbar c}$ and $N \in \mathbb{Z}$. The plateaus of the Hall conductivity are then identified with its classical values $\sigma_{xy} = n_e ec/B$ at concentrations n_e corresponding to an integer filling factor $n = n_e hc/eB$, that is, to an integer number of filled Landau levels. This consideration is further extended by the calculation of the Hall conductivity in the presence of disorder within Boltzmann[11] or self-consistent Born approximation,[13] i.e., for disorder-broadened Landau levels.

However, the spectral gaps in the density of states between separated Landau levels do not lead to the QHE. Indeed, while the dependence of the Hall conductivity on the Fermi energy is quantized in the clean system, this is not the true QHE. The point is that the Fermi level itself is not a smooth function of the density: it jumps between the fully occupied and empty Landau levels with increasing density. As a result, the density dependence of σ_{xy} (which is measured in experiments) shows up no steps and no plateaus, i.e., no QHE. Including the Landau level broadening by disorder leads only to the magneto-oscillations of $\sigma_{xy}(n_e)$ but not to its quantization.[14] In fact, (i) the QHE requires neither gaps nor pronounced oscillations of the density of states[15] of the disordered system and can even take place in systems without Landau levels;[16,17] (ii) the position of the QHE plateau transition does not necessarily correspond to the center of Landau level;[15,18] (iii) the crucial ingredient responsible for the Hall quantization is the disorder-induced Anderson localization[19,20] (for review, see Refs. 10, 21, and 22).

The existence of the odd-integer [Eq. (1)] QHE in graphene also requires a more rigorous justification in view of quantum interference effects that are essential in any two-dimensional system including graphene. Once disorder is fully taken into account, the quantization of Hall conductivity is exact and the transition between quantum Hall plateaus becomes a quantum phase transition with universal critical properties. This immediately shows the nonuniversality of the result (1). Indeed, if the disorder in graphene is of a generic form and does not possess any special symmetry, then the Dirac nature of excitations will be completely lost at large length scales. This is exactly what occurs in graphene with a generic (preserving only the global time-reversal symmetry) disorder at zero magnetic field B. In such a system, localization yields vanishing conductivity with lowering temperature.[23,24] The critical properties of the generically disordered graphene will not differ from those for any other two-dimensional system. The quantized Hall conductivity will then take all integer multiples of $2e^2/h$ rather than the odd series (1). Furthermore, $\sigma_{xy}=0$ at the Dirac point due to

the particle-hole symmetry. The conventional theory of the QHE[25] predicts complete localization in this situation. Specifically, any system with bare (Drude) Hall conductivity $(n-1/2)2e^2/h<\sigma_{xy}^{(0)}<(n+1/2)2e^2/h$ flows under renormalization group (RG) into localized fixed point with $\sigma_{xy}=n2e^2/h$, for any integer n including $n=0$. Hence, the Dirac point would be the center of a QH plateau with $\sigma_{xy}=0$ rather than a point of quantum Hall transition. Thus, the observation of the odd quantization [Eq. (1)] is a striking experimental result calling for theoretical explanation.

The only reason for a nonstandard quantization of the Hall conductivity is the presence of some special symmetry that is preserved by disorder and thus changes the critical behavior of the system. Unconventional transport and localization properties of graphene with special symmetries of disorder at $B=0$ were studied in Refs. 26 and 27 (see also earlier works on disordered Dirac fermions[16,28,29]). However, the quantum localization effects (and hence most of the peculiarities arising from the symmetry of disorder) were discarded in most analytical studies devoted to the QHE in graphene.[11,13,30,31] Recent numerical simulations of disordered graphene in magnetic field[32–34] have indeed shown that the result is sensitive to symmetry properties of disorder.

In this paper, we develop the theory of the integer QHE in graphene. We carry out the symmetry analysis and identify the situations when the QHE is anomalous. The structure of the article is as follows. In Sec. II, we consider QHE in monolayer graphene. After formulation of the model in Sec. II A, we turn to the analysis of different types of disorder. In Sec. II B, we consider the case of decoupled valleys and show the emergence of the odd QHE. In Sec. II C, we demonstrate that the valley mixing induces conventional QHE. An experimentally important case of Coulomb impurities, which lead to the crossover from odd to normal QHE with lowering temperature, is studied in Sec. II D. Section II E is devoted to disorder preserving the chiral symmetry of clean graphene resulting in a QHE peculiarity at the lowest Landau level. QHE in double-layer graphene is analyzed in Sec. III. Section IV summarizes our findings. Technical details are presented in Appendixes A and B. Appendix A contains calculation of density of states. The derivation of the effective field theory (sigma model) is the subject of Appendix B.

II. MONOLAYER GRAPHENE

A. Model and symmetries

We start with the effective Hamiltonian for the clean single-layer graphene in external magnetic field,

$$H=v_0\tau_3\boldsymbol{\sigma}\left(\mathbf{p}+\frac{e}{c}\mathbf{A}\right). \tag{2}$$

Here, the Pauli matrices σ_i and τ_i operate in the space of two sublattices, A and B, and two valleys, K and K', of the graphene spectrum, respectively. The full symmetry classification for this Hamiltonian in the absence of magnetic field was developed in Ref. 26. When the magnetic field is applied, time-inversion symmetry is broken and we are left with (i) an SU(2) isospin symmetry in the space of valleys[35] generated by $\Lambda_{x,y}=\sigma_3\tau_{1,2}$ and $\Lambda_z=\sigma_0\tau_3$ and (ii) an additional discrete chiral symmetry C_0 that exactly arises at zero energy: $H=-\sigma_3H\sigma_3$. Further, we denote $C_{x,y,z}$ the combinations of C_0 transformation with the isospin rotations.

We first consider the situation when all chiral symmetries are broken. This always happens when the Fermi energy is shifted away from the Dirac point by the gate voltage. At zero Fermi energy, the chiral symmetry can be violated by, e.g., any potential disorder. In this case, we have only two possibilities with respect to the symmetry: decoupled (Λ_z preserved) or mixed (Λ_z violated) valleys.

B. Decoupled valleys: Odd quantum Hall effect

We start with considering the case of decoupled valleys. A physical realization is any disorder smooth on the scale of lattice spacing. In particular, this situation would be realized if the random potential is due to impurities in the substrate separated by a thick (compared to the lattice constant) spacer from the graphene plane. The intervalley matrix elements of the disorder potential are then exponentially suppressed and can be safely neglected. The standard theoretical model for this type of disorder is the Gaussian random potential acting within a single valley. It is considered in Appendix A where we present the calculation of the density of states in magnetic field. The self-consistent Born approximation (SCBA) leads to Eq. (A7) for a nonzero Landau level and Eq. (A11) for the lowest Landau level. The fully controllable ballistic RG approach yields qualitatively similar results, Eqs. (A16) and (A24), respectively.

We address a more realistic case of long-range charged impurities directly located in the graphene plane, allowing for a weak intervalley scattering, in Sec. II D below. The scaling and universal behavior of both longitudinal and Hall conductivities is, however, independent of a particular disorder model. The degeneracy of a Landau level is lifted by any intravalley potential disorder while the isospin of electrons (valley index) is preserved. We will show that it is the isospin symmetry that is responsible for the odd quantization [Eq. (1)].

The isospin degeneracy implies the quantization of Hall conductivity with the step $4e^2/h$ (the factor of 4 accounts for 2 degenerate spin states and 2 independent valleys). Then, to prove the validity of Eq. (1), it suffices to establish the quantum Hall transition at zero filling. In order to do this, we make use of the low-energy theory (nonlinear sigma model[36]) for disordered graphene with decoupled valleys. For the case of zero magnetic field, this theory was derived in Ref. 27 (see also Refs. 23, 24, and 37). The derivation allowing for magnetic field is given in Appendix B. The model is separated into two independent sectors corresponding to the two valleys. In each sector, the action has the form

$$S[Q]=\frac{1}{4}\mathrm{Str}\left[-\frac{g_{xx}}{2}(\nabla Q)^2+\left(g_{xy}\pm\frac{1}{2}\right)Q\nabla_xQ\nabla_yQ\right]. \tag{3}$$

The field Q is the 4×4 supermatrix operating in Fermi–Bose and advanced-retarded spaces. The two parameters of the model, g_{xx} and g_{xy}, are longitudinal and Hall conductivities per one valley and per spin component measured in units

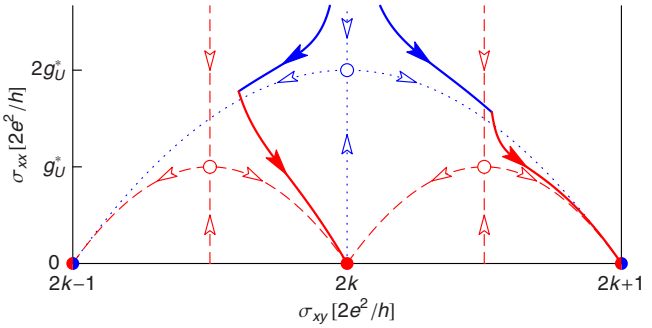

FIG. 1. (Color online) Renormalization group flow of σ_{xx} and σ_{xy} in graphene with decoupled and mixed valleys. Dotted (dashed) lines are separatrices of the flow for graphene with decoupled (mixed) valleys. Open circles are unstable fixed points corresponding to quantum Hall transitions. Stable fixed points (plateaus) are shown as disks. Two solid curves demonstrate a possible flow toward even- and odd-plateau fixed point for a model with weakly mixed valleys. Each curve has a cusp when the running scale reaches l_{mix}.

e^2/h. The "Str" operation implies the supertrace in all indices of the matrix along with real-space integration. This action differs from the usual sigma model in quantizing magnetic field[25] by the addition of $\pm 1/2$ to g_{xy}. This additional contribution arises due to the quantum anomaly of Dirac fermions.[17,27,29] It is the only reminiscent of the Dirac nature of excitations that survives at large scales and influences the critical properties. The signs in front of the anomalous terms $1/2$ are opposite for the two valleys. This ensures the global parity symmetry ($x \mapsto -x$, $K \mapsto K'$) of the total action.

The second term of the action (3) has a topological nature: $\mathrm{Str}(Q\nabla_x Q \nabla_y Q) \equiv 8i\pi N[Q]$ with $N[Q]$ taking only integer values. This term gives the imaginary part of the action $\mathrm{Im}\, S[Q] = \theta N[Q]$ with the vacuum angle $\theta = 2\pi g_{xy} \pm \pi$.

The initial values of g_{xx} and g_{xy} are determined by the corresponding Drude expressions [see Eqs. (B6), (B10), (B12), and (B16)]. The quantum corrections that establish localization and, hence, the QHE are the result of renormalization of the action (3). The renormalization flow of g_{xx} and θ was proposed in Refs. 25 and 38. We schematically plot this flow in Fig. 1 by dotted lines. The effective theory [Eq. (3)] is invariant with respect to the vacuum angle shift $\theta \mapsto \theta + 2\pi$; hence, the flow pattern is a periodic function of g_{xy}. Transitions between quantum Hall plateaus occur when the value of θ passes through an odd multiple of π. Due to the anomalous contribution in Eq. (3), this is the case at zero filling factor when $g_{xy}=0$. Thus, we have shown the validity of the odd quantization series (1) in the case when *disorder does not mix the valleys*. The absence of anomaly would have led to a plateau rather than the transition at $n=0$ similarly to ordinary QHE.

Physically, the step of Hall conductivity between plateaus is due to a critical delocalized state, which is exactly at the Fermi energy when $\theta = \pi$. All other states are localized and do not contribute to either longitudinal or Hall conductivity. The value of longitudinal conductivity exhibits a peak at the transition point with the maximum value

$$\sigma_{xx} = 4g_U^* \approx 2e^2/h, \tag{4}$$

where g_U^* is the longitudinal conductivity for the ordinary quantum Hall effect (known to be in the range $g_U^* \simeq 0.5-0.6$ from numerical simulations[39]) and the factor of 4 again reflects the valley and spin degeneracy. Equation (4) agrees with the experimental value found in the strong magnetic field at the Dirac point.[4,5,8]

C. Mixed valleys: Ordinary quantum Hall effect

Let us now turn to the case when a weak valley mixing is present. For instance, charged impurities scatter electrons between valleys at some small rate τ_{mix}^{-1}, as compared to the intravalley scattering rate τ^{-1}. The total action of the system will then be perturbed by the small coupling between matrices Q_K and $Q_{K'}$ corresponding to the two valleys (see Appendix B 2 for the derivation),

$$S[Q_K, Q_{K'}] = S[Q_K] + S[Q_{K'}] + \frac{\hbar\rho}{\tau_{\mathrm{mix}}} \mathrm{Str}\, Q_K Q_{K'}, \tag{5}$$

where $S[Q_{K,K'}]$ is given by Eq. (3) and ρ is the density of states at the Fermi level (see Appendix A). This perturbation is relevant and leads to the constraint $Q_K = Q_{K'}$ in the infrared limit. The corresponding valley-mixing length is determined by the relation $l_{\mathrm{mix}}/l \sim (\tau_{\mathrm{mix}}/\tau)^{1/z}$. The ultraviolet scales l and τ are given by the effective mean free path and time; in strong magnetic field (for low-lying Landau levels with $|N| \sim 1$), the length l is of the order of the magnetic length, $l \sim l_B = \sqrt{\hbar c/eB}$, and the mean free time $\tau \sim \hbar l_B^2 \rho$. The index is $z=2$ for noninteracting electrons (diffusion propagation) and in the case of short-range interaction.[40] A different value of z emerges in the case of Coulomb interaction;[41] experiments[42] yield $z \simeq 1$.

At a scale larger than l_{mix}, we have $Q_K = Q_{K'}$ and the topological terms with anomalous factors $\pm 1/2$ cancel in Eq. (5). We end up with the unitary sigma model for the *normal* QHE[24] with $\theta = 4\pi g_{xy}$ and ordinary quantization of Hall conductivity,

$$\sigma_{xy} = k2e^2/h, \quad k \in \mathbb{Z}. \tag{6}$$

A delocalized state at the center of each Landau level is doubly degenerate when the valleys are decoupled. A weak valley mixing leads to a small splitting of the delocalized state *within a single broadened Landau level*. The new even plateau appears between the two odd ones when the chemical potential lies between the two split delocalized states (see Fig. 2). The longitudinal conductivity σ_{xx} has two separated peaks $2g_U^* \simeq e^2/h$ in this case (here the factor of 2 is due to the spin degeneracy). It is worth mentioning a similarity of the splitting of the anomalous QHE and the splitting of delocalized states by spin-orbit (spin-flip) scattering in a spin-degenerate ordinary QHE.[15,43]

The flow of σ_{xx} and σ_{xy} for both cases of decoupled and mixed valleys is shown in Fig. 1. For weakly mixed valleys (solid lines), a crossover occurs between these two flows at the length l_{mix}. The even plateaus are much shorter than the odd ones [Eq. (1)] provided that the valley mixing is weak. If

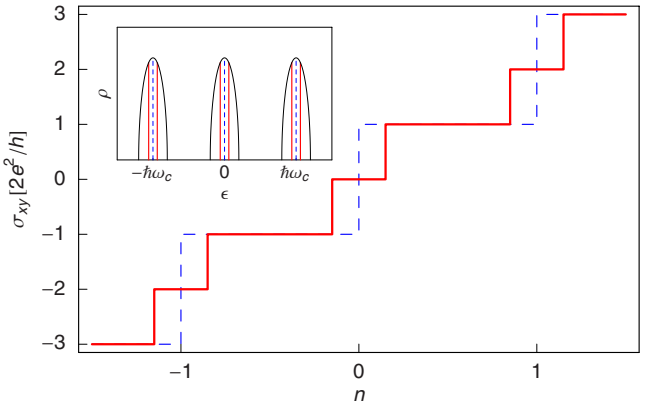

FIG. 2. (Color online) Quantum Hall effect in graphene with smooth disorder at zero temperature. Hall conductivity as a function of the filling factor: odd (decoupled valleys, dashed line) vs normal (weak valley mixing, solid line) quantization. The inset shows the energy dependence of the density of states. The state in the center of Landau level is delocalized (dashed lines) when the valleys are decoupled. The valley mixing splits this delocalized state (solid lines).

the valleys are completely decoupled, the quantum Hall transition between two successive odd plateaus has a finite width determined by the temperature-dependent dephasing length l_φ. The states close to the center of Landau level are localized at length that diverges as $l_{\mathrm{loc}} \sim l(\delta n)^{-\nu}$, where δn is the deviation of the filling factor $n = 2\pi l_B^2 n_e$ from the transition point and $\nu \simeq 2.3$ is the conventional quantum Hall critical index. The width of the transition is then $\delta n \sim (l/l_\varphi)^{1/\nu}$. If the valley-mixing length l_{mix} is larger than l_φ, the even plateaus will be totally smeared—the splitting between critical states is smaller than the delocalized energy region around them. The even plateau becomes visible at sufficiently low T when l_φ exceeds l_{mix} (see Fig. 3). Therefore, the width of this new plateau is

$$\delta n_{\mathrm{even}} \sim \delta n(l_\varphi = l_{\mathrm{mix}}) \sim (l/l_{\mathrm{mix}})^{1/\nu} \sim (\tau/\tau_{\mathrm{mix}})^{1/\nu z}. \quad (7)$$

Recent numerical studies[32] demonstrated the splitting of quantum Hall transition in graphene with a combination of

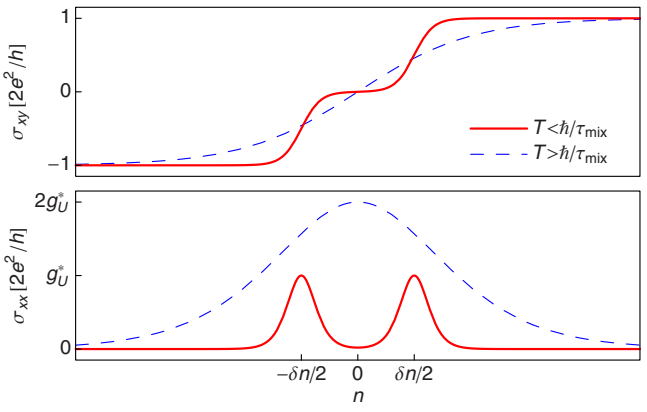

FIG. 3. (Color online) Quantum Hall transition at finite temperature. A double step in σ_{xy} and a double peak in σ_{xx} (solid lines) require low temperature, $T \lesssim \hbar/\tau_{\mathrm{mix}}$. Otherwise, a single broadened quantum Hall transition is seen (dashed lines).

potential and bond disorder. At the same time, the model with only potential disorder was found to show only the odd QHE in Ref. 32. On the contrary, our consideration yields the existence of even plateaus in this case but with a narrower plateau at zero filling factor [see Eqs. (B20), (B22), and (11)]. The zeroth plateau arises due to Landau level mixing which was discarded in Ref. 32.

Two other mechanisms, apart from intervalley scattering, can establish the even quantum Hall plateaus, Zeeman splitting, and electron-electron interaction. Zeeman effect is weak in graphene; however, in Ref. 8, the zero plateau that emerged in the high magnetic field was attributed to this mechanism. An alternative—Stoner—mechanism was advocated in Ref. 6. Indeed, the repulsive interaction between electrons may result in the Stoner instability[44–46] giving rise to spontaneous breaking of spin and/or valley symmetry. Let us note that this instability would completely split the Landau level leading to the formation of even quantum Hall plateaus with the width comparable to that of odd plateaus as the magnetic field or electron mobility is increased.[44,45] At the same time, the splitting of QH transition due to valley mixing is independent of the magnetic field. This can be used to experimentally distinguish the Stoner splitting from the disorder-induced splitting analyzed in the present work.

D. Coulomb impurities: Anomalous-normal quantum Hall effect crossover

So far, we have considered the most general situation not specifying the disorder model. We have shown that arbitrary small valley mixing leads to the normal QHE (with even plateaus) at zero temperature. Smooth disorder with finite correlation length produces an exponentially weak intervalley coupling and hence exponentially low temperature is required to observe the normal QHE.

In this section, we address the case of long-range charged impurities. This model appears to be most relevant for graphene experiments because it conforms with both linear dependence of conductivity on the concentration of electrons[44] and with minimal conductivity at the Dirac point.[47] Due to the $1/r$ singularity of Coulomb potential at short distances, the amplitude of intervalley scattering is suppressed only in the power-law fashion. Thus, the temperature of anomalous-normal QHE crossover $[\tau_\phi(T) \sim \tau_{\mathrm{mix}}]$ is expected to be experimentally accessible.

Disorder due to charged impurities can be treated in the framework of SCBA developed in Appendix A 1 once the screening is taken into account. For low-lying Landau levels, the screening length is of the order of magnetic length, which is the only scale in the magnetic field.[44] For high Landau levels, the screening occurs at a scale of the electron wavelength. If the dimensionless parameter characterizing the interaction strength is small, $r_s = e^2/v_0\chi \ll 1$ (χ is the dielectric constant), the screening can be controllably treated within the random phase approximation. In a more realistic situation, $r_s \sim 1$, the results for charged impurities are valid up to a numerical factor of order unity in the definition of the effective Born parameter,

$$\alpha \sim n_{\mathrm{imp}} l_B^2 \begin{cases} 1/N, & N \neq 0 \\ 1, & N = 0. \end{cases} \quad (8)$$

Here, n_{imp} is the concentration of impurities.

The density of states has the form of Eq. (A16) with the above value of α and with $Z=1$. The absence of energy rescaling is due to the suppression of scattering off Coulomb impurities with large momentum transfer (that is, transitions involving far Landau levels are ineffective). The lack of hard scattering also leaves no room for ballistic renormalization described in Appendix A 2. The width of Landau level peak gives the intravalley scattering rate

$$\tau^{-1} \sim \omega_c \sqrt{\alpha} \sim v_0 n_{\mathrm{imp}}^{1/2} \begin{cases} 1/N, & N \neq 0 \\ 1, & N = 0. \end{cases} \tag{9}$$

Note that at zero energy ($N=0$), the mean free time is independent of the magnetic field.

Intervalley scattering involves large momentum transfer. This allows us to neglect screening and estimate the corresponding parameter as

$$\beta_\perp \sim n_{\mathrm{imp}} a^2, \tag{10}$$

where a is the lattice constant. The microscopic calculation of τ_{mix} within both SCBA and ballistic RG approaches is presented in Appendix B 2. The valley-mixing rate due to Coulomb impurities follows from any of Eq. (B20) or (B22) with logarithmic factors replaced by numbers of order unity,

$$\frac{\tau_{\mathrm{mix}}}{\tau} \sim \begin{cases} \alpha/\beta_\perp \sim l_B^2/a^2 N, & N \neq 0 \\ \beta_\perp^{-1} \sim (n_{\mathrm{imp}} a^2)^{-1}, & N = 0. \end{cases} \tag{11}$$

Taking a typical magnetic field value of 20 T, we get $\delta n_{\mathrm{even}} \sim (a^2 N / l_B^2)^{0.4} \sim 10\%$ splitting of quantum Hall transitions for low-lying Landau levels. A smaller splitting of order $\delta n_{\mathrm{even}} \sim (n_{\mathrm{imp}} a^2)^{0.4} \sim 5\%$ appears at zero Landau level if we estimate $n_{\mathrm{imp}} \sim 4 \times 10^{11}$ cm^{-2} from mobility measurements away from the Dirac point.[4]

In experiment, the temperature should be low enough in order to resolve the quantum Hall transition splitting, $T \lesssim \hbar / \tau_{\mathrm{mix}}$. This implies $T \lesssim 100$ mK for the lowest Landau level and $T \lesssim 1$ K for higher levels. These values are in reasonable agreement with weak localization measurements in the low magnetic field.[48] At higher temperatures, a broadened double step of Hall conductivity will be seen instead of two split transitions (Fig. 3).

We now briefly comment on the connection of the above results with the universal minimal conductivity[1] near the Dirac point in zero magnetic field. The scattering rate near the Dirac point[26,44,49] is $\tau^{-1} \sim v_0 n_{\mathrm{imp}}^{1/2}$ in agreement with Eq. (9). The intervalley processes occur with a much smaller rate $\tau_{\mathrm{mix}}^{-1} \sim v_0 n_{\mathrm{imp}}^{3/2} a^2$, see Eq. (11) above. When the temperature is as low as $\hbar / \tau_{\mathrm{mix}}$, the intervalley scattering becomes crucial and leads to strong localization (orthogonal symmetry class).[23] According to the above estimate, this temperature is ~ 100 mK (for $n_{\mathrm{imp}} \approx 4 \times 10^{11}$ cm^{-2}), which is accessible in modern experiments.[50] When the purity of samples is improved, τ_{mix}^{-1} at zero energy decreases as $n_{\mathrm{imp}}^{3/2}$ shifting the crossover to localization and to normal QHE toward lower temperatures.

Experimental observation of linear conductivity dependence on the carrier concentration[7] strongly favors the disorder model due to Coulomb impurities[26,44,49] and/or ripples.[51,52] We have shown that Coulomb impurities are also consistent with the anomalous (odd) quantization of Hall conductivity [Eq. (1)]. The same is true when Coulomb impurities are accompanied by ripples. If the dominant randomness in the system is due to ripples, the QHE will exhibit additional anomalies studied below.

E. Chiral disorder: "Classical" quantum Hall effect

So far, we have considered the situation of a generic disorder within each valley. In Ref. 26, it was shown that once the chiral symmetry C_0 is preserved by the disorder (e.g., ripples), the longitudinal conductivity at zero energy is exactly $4e^2/\pi h$. External magnetic field also does not violate the chiral symmetry and hence does not change the value of conductivity.[53] This leads us to the conclusion that the quantum Hall transition occurring at zero filling factor is modified by the presence of C_0 symmetry since $\sigma_{xx} = 4e^2/\pi h$ differs from the universal value [Eq. (4)] characteristic for a normal quantum Hall transition, $\sigma_{xx} \approx 2e^2/h$.

A general form of chiral disorder in a single valley is a random (Abelian) vector potential $\mathbf{A}(\mathbf{r})$. The zeroth Landau level remains exactly degenerate in this situation,[54] as follows from the Atiyah–Singer theorem.[55] Moreover, one can explicitly find the wave functions at zero energy. After a proper gauge transformation, any two-dimensional vector potential can be expressed as a curl of a scalar field $\phi(\mathbf{r})$,

$$A_x = -\nabla_y \phi, \quad A_y = \nabla_x \phi. \tag{12}$$

This field ϕ is uniquely determined by the magnetic field $B(\mathbf{r})$ penetrating the system, $\nabla^2 \phi = -B$. Assume that the uniform part of magnetic field B_0, the one that establishes Landau levels, is pointing up, $B_0 > 0$. Then, the function ϕ grows at infinity as $\phi \sim B_0 r^2$ and all the zero-energy wave functions entirely lie in sublattice B. A possible set of such functions (up to a normalization factor) is

$$\Psi_m^B(x,y) = (x - iy)^m \exp(-e\phi/\hbar c). \tag{13}$$

Exact degeneracy of the Landau level implies the absence of localization. When the chemical potential lies at zero energy, the system exactly behaves as if it were clean. This means that the Hall effect is *classical* rather than quantum with a linear dependence of Hall conductivity on electron concentration n_e,

$$\sigma_{xy} = n_e e c / B = n 4e^2/h. \tag{14}$$

This classical dependence holds for filling factor within the zeroth Landau level, $|n| < 1/2$. The longitudinal conductivity remains constant, $\sigma_{xx} = 4e^2/\pi h$, in this case. The behavior of the Hall conductivity is shown in Fig. 4.

Let us now include a weak valley mixing maintaining the C_0 chiral symmetry. For instance, this is the case when the main disorder due to ripples is accompanied by rare dislocations. Let us recall that in the case of random scalar potential, the intervalley mixing leads to the splitting of the quantum Hall transition into two with a small $\sigma_{xy} = 0$ plateau in between. The longitudinal conductivity is zero in this case. One could thus expect a similar behavior for chiral disorder. However, the conductivity at $n=0$ remains $4e^2/\pi h$ according to the result of Ref. 26 as long as the chiral symmetry is preserved. This implies no QHE plateau.

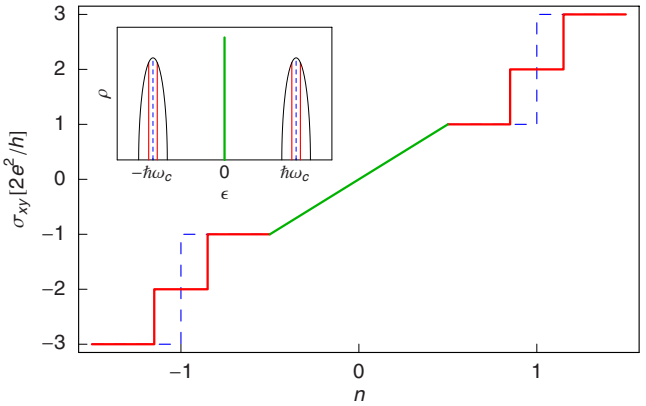

FIG. 4. (Color online) "Classical" QHE in graphene with chiral disorder (random vector potential). Chiral symmetry protects degeneracy of the lowest Landau level (inset: delta-function in the density of states). Hall conductivity is a linear function of carrier concentration while the lowest Landau level is being filled. In Abelian case (ripples), only odd plateaus appear away from zero energy (dashed line). Non-Abelian gauge disorder (dislocations) split quantum Hall transitions as shown by solid line.

How does it happen that the valley mixing does not induce a quantum Hall plateau around the Dirac point? The answer is the same as for the Abelian random vector potential discussed above: the zeroth Landau level remains exactly degenerate. The disorder we consider corresponds to a random *non-Abelian* vector potential $\mathbf{A}(\mathbf{r})$, which is a matrix in the valley space. The degeneracy of the $N=0$ Landau level is a direct corollary of the Atiyah–Singer theorem.[55] An explicit construction of zero-energy wave functions is almost the same as above:[56] express the vector potential in the form

$$A_+ = \frac{i\hbar c}{e} g^{-1}\partial_+ g, \quad A_- = -\frac{i\hbar c}{e} g\partial_- g^{-1}, \tag{15}$$

where $A_\pm = A_x \pm iA_y$, $\partial_\pm = \nabla_x \pm i\nabla_y$, and g is an appropriate 2×2 matrix in the valley space. The wave functions of the zeroth Landau level again lie in sublattice B and have the form

$$\Psi_m^B(x,y) = (x-iy)^m g_{1,2}, \tag{16}$$

with $g_{1,2}$ being any of the two columns of the matrix g.

The Hall conductivity again *classically* behaves within the zeroth Landau level, $\sigma_{xy}=4ne^2/h$ for $|n|<1/2$, but the other quantum Hall transitions, away from $n=0$, split into pairs with narrow plateaus in between (see Fig. 4), in the case of weakly mixed valleys.

The observation of a narrow quantum Hall transition in graphene at $n=0$ seems to indicate that the dominant scattering mechanism is provided by long-range potential impurities rather than by ripples or dislocations. This is in agreement with the observed value of the zero-B minimal conductivity at the Dirac point, which is appreciably larger than $4e^2/\pi h$ expected for a random vector potential. On the other hand, very recent experimental study of quantum Hall gaps in graphene[57] revealed that the lowest Landau level is significantly narrower than other Landau levels. This can be a signature of preserved chiral symmetry, suggesting that the main scattering mechanism is due to ripples in the samples studied in Ref. 57. The quantum Hall measurement would provide a powerful test of this conjecture.

III. DOUBLE-LAYER GRAPHENE

Let us turn to the QHE in double-layer graphene. We limit our consideration to the case of disorder which does not mix the two valleys. The single-valley Hamiltonian of double-layer graphene reads[58]

$$H = \frac{1}{2m}[\sigma_x(p_x^2 - p_y^2) + 2\sigma_y p_x p_y]. \tag{17}$$

The Landau levels are $\epsilon_N = \hbar\omega_c\sqrt{N(N-1)}$ with the conventional definition of cyclotron frequency $\omega_c = eB/mc$. The two lowest levels, $N=0$ and $N=1$, are degenerate. The corresponding wave functions are spinors in the sublattice space: $(0,\psi_0)^T$ and $(0,\psi_1)^T$, respectively, where ψ_N is the wave function of the Nth Landau level in a normal metal.

In the presence of a generic disorder within each valley, we have the same action (3) but with doubled couplings. The anomalous contribution to the topological term gives now $\theta=2\pi$ rather than π at zero energy. This implies complete localization and, hence, a plateau at $n=0$. However, in experiments, a plateau transition with the double step in σ_{xy} at $n=0$ is observed instead. This can only happen if the disorder does not mix the two degenerate Landau levels with $N=0$ and $N=1$. The only possible reason of the lack of mixing is the smoothness of disorder on the scale of magnetic length $l_B=\sqrt{\hbar c/eB}$. Indeed, the wave functions of the two Landau levels are orthogonal and concentrated in the area of order l_B^2. If the disorder potential is almost constant in this small region, the corresponding matrix element is suppressed due to the orthogonality of wave functions. More specifically, assuming the disorder correlation length $d \gg l_B$, the mixing rate of the two Landau levels is found as $\tau_{01}^{-1} \sim \tau^{-1}(l_B/d)^2$. Comparison of τ_{01} with the time needed for localization gives us the width of the zeroth plateau (see Fig. 5),

$$\delta n_0 \sim (l_B/d)^{2/\nu z}. \tag{18}$$

To resolve this plateau, one should satisfy an upper bound on temperature, $T \lesssim \hbar/\tau_{01}$.

It is worth noting that the experimentally measured double step of the Hall conductivity at $n=0$ cannot be automatically explained by the charged impurities in graphene. A random potential due to charged impurities has no characteristic length d. The only scale associated with such disorder is the screening length that is of the order of l_B (the stronger is the magnetic field, the larger is the density of states in Landau level, and the more efficient is the screening).[44] The experimental observation of the double step in double-layer graphene thus suggests that an additional scale exists, characterizing the smoothness of disorder. It might be caused by impurity correlations or, else, by their separation from the graphene layer.

So far, we have considered the QHE in a single valley of a double-layer sample. If we include an intervalley scattering in our model, then the $4e^2/h$ quantum Hall steps will further

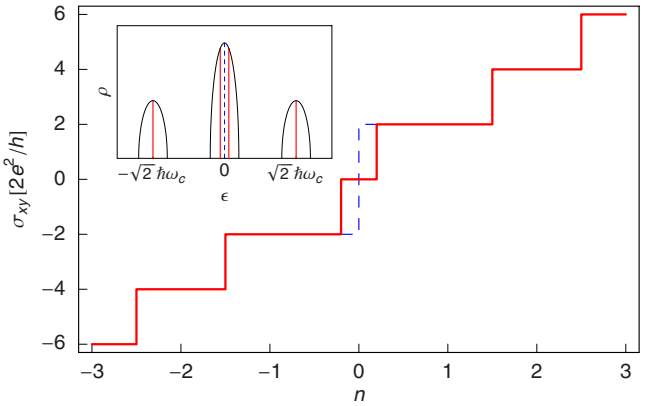

FIG. 5. (Color online) QHE in a double-layer graphene with smooth disorder (decoupled valleys). Degeneracy of the lowest Landau level is twice larger than for other levels. Double step at zero filling factor (dashed line) is split when the disorder has finite correlation length d. The inset shows the density of states and positions of delocalized states (solid lines). Two such states within the lowest Landau level remain degenerate (dashed line) in the limit $d\to\infty$.

split, similarly to single layers studied above. As a result, the conventional QHE with $2e^2/h$ steps will be fully restored.

IV. SUMMARY

In this paper, we have developed the theory of integer QHEs in graphene. The Landau level structure by itself is not sufficient to determine the form of the QHE. Anomalous QHEs in graphene are due to the special character (symmetry) of disorder, in particular:

(i) A smooth random (scalar) potential, which does not couple the valleys, gives rise to the odd QHE [Eq. (1) and dashed line in Fig. 2].

(ii) The valley mixing splits the odd quantum Hall transitions and restores the ordinary Hall quantization [Eq. (6) and solid line in Fig. 2].

(iii) For weakly mixed valleys, the crossover from odd to ordinary QHE occurs at parametrically low temperatures. A particularly relevant example of weak valley mixing is provided by Coulomb impurities. For realistic concentration of impurities, the crossover temperature is experimentally accessible, $T\lesssim\tau_{\rm mix}^{-1}\sim 100$ mK.

(iv) Ripples or dislocations (random vector potential preserving the chiral symmetry) lead to a "classical" QHE [Eq. (14) and Fig. 4] around the half filling.

(v) In double layers, a double-step QHE transition at $n=0$ arises for disorder smooth on the scale of l_B.

Experiments on QHE in graphene thus provide information about the nature of disorder. The observation of the odd QHE indicates the long-range type of disorder. The absence of localization in zero magnetic field and linear behavior of conductivity with the gate voltage favors the model of Coulomb impurities possibly accompanied by ripples.

ACKNOWLEDGMENTS

We are grateful to K. S. Novoselov, L. S. Levitov, D. G. Polyakov, and A. K. Savchenko for valuable discussions. The work was supported by the Center for Functional Nanostructures of the Deutsche Forschungsgemeinschaft. The work of I.V.G. was supported by the EUROHORCS/ESF EURYI Awards scheme.

APPENDIX A: DISORDERED GRAPHENE IN STRONG MAGNETIC FIELD

Here, we present the calculation of the averaged Green function and of the density of states in disordered graphene in the presence of a strong external magnetic field. We will use the results of this calculation below for the derivation of the nonlinear sigma model. We assume $\hbar=1$ from now on.

1. Self-consistent Born approximation

Let us start with the SCBA approach. We assume single-layer graphene with Gaussian δ-correlated disorder and consider first the simplest case of potential disorder characterized by a dimensionless coupling constant α (it corresponds to α_0 in Ref. 26). This type of disorder does not produce any valley mixing, so that we can use the single-valley Hamiltonian. Intervalley scattering processes will be included later.

For the single-valley case, the Green function is a 2×2 matrix in the sublattice space. In the presence of magnetic field, the disorder-induced self-energy matrix has two distinct components, $\Sigma_{1,2}$, yielding the Green function

$$G(\epsilon)=\begin{pmatrix}\epsilon_1 & v_0\hat{\pi}_-\\ v_0\hat{\pi}_+ & \epsilon_2\end{pmatrix}^{-1},\quad \hat{\pi}_\pm=p_x\pm ip_y+\frac{e}{c}(A_x\pm iA_y),$$

where $\epsilon_{1,2}=\epsilon-\Sigma_{1,2}$.

The calculation of inverse matrix is straightforward in the basis of Landau levels. Due to the fact that the disorder is δ correlated, the SCBA equation involves only the Green function at coincident points. The latter is independent of a particular gauge and reads

$$G(\epsilon;\mathbf{r},\mathbf{r})=\frac{\omega_c^2}{4\pi v_0^2}\begin{pmatrix}\epsilon_2\sum_{N'=1}^{\infty} & 0\\ 0 & \epsilon_1\sum_{N'=0}^{\infty}\end{pmatrix}\frac{1}{\epsilon_1\epsilon_2-\omega_c^2N'}. \tag{A1}$$

The matrix SCBA equation $\Sigma(\epsilon)=2\pi v_0^2\alpha G(\epsilon;\mathbf{r},\mathbf{r})$ determines two self-energies $\Sigma_{1,2}$,

$$\begin{Bmatrix}\Sigma_1\\ \Sigma_2\end{Bmatrix}=\frac{\alpha\omega_c^2}{2}\begin{Bmatrix}\epsilon_2\sum_{N'=1}^{\infty}\\ \epsilon_1\sum_{N'=0}^{\infty}\end{Bmatrix}\frac{1}{\epsilon_1\epsilon_2-\omega_c^2N'}. \tag{A2}$$

This equation was numerically analyzed in Ref. 12. In the absence of magnetic field, the sum over Landau levels replaces by the integral and the well-known graphene SCBA equation is reproduced.[59]

We are interested in the case of strong magnetic field when Landau levels are well separated. Let us focus on a particular Nth level. Although SCBA gives the exact shape of the density of states only for $N \gg 1$, it yields a parametrically correct estimate for the height and width of the Landau level peak for all N.

Consider first the case $N \neq 0$. Then, the largest term in the sums in Eq. (A2) is the one with $N'=N$. We estimate the sum of all other terms by replacing it with the corresponding integral. (It is worth noting that contrary to the case of a normal metal, the contribution of far Landau levels with $N' \neq N$ cannot be neglected. In graphene, the density of states linearly grows with energy; in the strong magnetic field, this leads to Landau level separation decreasing as $\omega_c/\sqrt{N'}$. As a result, the contribution from high Landau levels to the self-energy should be retained.) The difference between Σ_1 and Σ_2, which originates from the term with $N'=0$ in Eq. (A2), is immaterial for $N \neq 0$; we will use a unified notation Σ for them. We further simplify the equation by employing the inequality $|\epsilon - \epsilon_N|, |\Sigma| \ll \epsilon_N$ and obtain

$$\Sigma = \frac{\alpha\omega_c^2}{4(\epsilon - \epsilon_N - \Sigma)} - \alpha(\epsilon - \Sigma)\ln\frac{\Delta}{\epsilon_N}. \tag{A3}$$

The logarithmic divergence is cut by the graphene bandwidth Δ.

The effect of magnetic field is encoded in the ω_c^2 term in Eq. (A3). If this term were absent, the result would reproduce the well-known disorder-driven renormalization of the energy,[26]

$$\tilde{\epsilon} = \epsilon - \mathrm{Re}\,\Sigma_0 = \epsilon/Z, \quad Z = 1 - \alpha\ln(\Delta/\epsilon_N). \tag{A4}$$

It is instructive to express the solution of the full equation (A3) in terms of this renormalized energy $\tilde{\epsilon}$,

$$\epsilon - \Sigma = \frac{\tilde{\epsilon} + \epsilon_N}{2} \pm i\sqrt{\tilde{\gamma}^2 - \left(\frac{\tilde{\epsilon} - \epsilon_N}{2}\right)^2}. \tag{A5}$$

The appeared parameter $\tilde{\gamma}$ determines the imaginary part of the self-energy in the center of Landau level,

$$\tilde{\gamma} = \frac{\omega_c\sqrt{\alpha}}{2\sqrt{1 - \alpha\ln(\Delta/\epsilon_N)}}. \tag{A6}$$

The density of states within each Landau level has a standard form of semicircle. The identity $\rho(\epsilon) = -\pi^{-1}\,\mathrm{Im}\,\mathrm{tr}G^R(\epsilon;\mathbf{r},\mathbf{r})$ together with the self-consistency equation yields

$$\rho(\epsilon) = \mathrm{Im}\,\frac{\Sigma_1 + \Sigma_2}{2\pi^2 v_0^2 \alpha} = \frac{\sqrt{4\tilde{\gamma}^2 - (\tilde{\epsilon} - \epsilon_N)^2}}{2\pi^2 v_0^2 \alpha} = \frac{\sqrt{4\gamma^2 - (\epsilon - \epsilon_N Z)^2}}{4\pi^2 l_B^2 \gamma^2}. \tag{A7}$$

The last expression contains two parameters: the renormalization factor Z determines the rescaling of Landau levels according to Eq. (A4) and the electron scattering rate $\gamma = \tilde{\gamma}Z$ gives the Landau level width.

The result (A7) together with Eq. (A6) provides the following criterion for the separation of Landau levels within SCBA: the Nth level becomes isolated when $\omega_c Z/\sqrt{N} \gtrsim \gamma$. The stronger is the magnetic field, the larger is the number of isolated Landau levels in the vicinity of the Dirac point.

The solution of the SCBA equation is qualitatively different for the lowest Landau level, $N=0$. The distinction between Σ_1 and Σ_2 is now crucial since the term with $N'=0$ is absent in the sum (A2) for Σ_1. By replacing the sums over nonzero levels with the integrals, we get

$$\Sigma_1 = -\alpha(\epsilon - \Sigma_2)\ln(\Delta/\omega_c),$$
$$\Sigma_2 = \frac{\alpha\omega_c^2}{2(\epsilon - \Sigma_2)} - \alpha(\epsilon - \Sigma_1)\ln(\Delta/\omega_c). \tag{A8}$$

We express the solution of these equations in terms of renormalized energy $\tilde{\epsilon}$ according to Eq. (A4),

$$\epsilon - \Sigma_2 = \frac{\tilde{\epsilon}}{2} \pm i\sqrt{\tilde{\gamma}_2^2 - \frac{\tilde{\epsilon}^2}{4}},$$
$$\Sigma_1 = -\alpha\ln(\Delta/\omega_c)\left[\frac{\tilde{\epsilon}}{2} \pm i\sqrt{\tilde{\gamma}_2^2 - \frac{\tilde{\epsilon}^2}{4}}\right]. \tag{A9}$$

We denote the imaginary parts of $\Sigma_{1,2}$ at the center of Landau level by $\tilde{\gamma}_{1,2}$,

$$\begin{Bmatrix}\tilde{\gamma}_1\\ \tilde{\gamma}_2\end{Bmatrix} = \begin{Bmatrix}\alpha\ln(\Delta/\omega_c)\\ 1\end{Bmatrix}\frac{\omega_c\sqrt{\alpha}}{\sqrt{2[1 - \alpha^2\ln^2(\Delta/\omega_c)]}}. \tag{A10}$$

The electron scattering rates for the two sublattices are given by $\gamma_{1,2} = Z\tilde{\gamma}_{1,2}$ with Z from Eq. (A4). The rate γ_2 has the same order of magnitude as for a nonzero Landau level [Eq. (A6)], while γ_1 is somewhat smaller. This is a manifestation of the fact that the lowest Landau level wave function has its support in sublattice B. With the opposite orientation of magnetic field, the wave function will be in sublattice A and $\gamma_1 > \gamma_2$. In the second valley, the situation is reversed.

By calculating the density of states at the lowest Landau level separately for two sublattices, we find

$$\begin{Bmatrix}\rho_1\\ \rho_2\end{Bmatrix} = \begin{Bmatrix}\alpha\ln(\Delta/\omega_c)\\ 1\end{Bmatrix}\frac{\sqrt{4\gamma^2 - \epsilon^2}}{4\pi^2 v_0^2 \alpha Z}. \tag{A11}$$

For both sublattices, the width of the zeroth Landau level is $\gamma = \tilde{\gamma}_2 Z$, which determines the width of the total density of states $\rho = \rho_1 + \rho_2$.

2. Ballistic renormalization group

As we discussed in the previous section, high Landau levels produce logarithmic corrections to the low-energy properties of the system. The SCBA takes these corrections into account only partially. The systematic way for summing up such logarithms is the renormalization group (RG) formalism.[16,23,26,28,29] Below, we develop this approach for the case of strong magnetic field. As we demonstrate, the results are qualitatively similar to the SCBA but quantitatively differ.

In the simplest case of diagonal Gaussian disorder α, the starting point for the renormalization group is the fermionic action

$$S[\psi] = \int d^2r[-i\bar{\psi}(\epsilon + i0\Lambda - H)\psi + \pi v_0^2 \alpha(\bar{\psi}\psi)^2]. \tag{A12}$$

Here, H is the single-valley Dirac Hamiltonian. The field ψ is an 8-supervector with the structure in the inner AB space (sublattices) of the Hamiltonian H, retarded-advanced (RA) space, and Bose–Fermi (BF) superspace.[23,27] We use standard notation $\Lambda = \mathrm{diag}\{1,-1\}_{RA}$. The doubling of variables in the RA space is needed for the calculation of averages involving both retarded and advanced Green functions, e.g., conductivity. In the ballistic regime that we consider here, the distinction between retarded and advanced propagators is immaterial.

The renormalization procedure eliminates fast degrees of freedom, thus reducing the cutoff energy $\Delta \to \Delta/L$. The parameters of the action (A12) are then rescaled according to[26]

$$\frac{d\alpha}{d\ln L} = 2\alpha^2, \quad \frac{d\epsilon}{d\ln L} = \alpha\epsilon. \tag{A13}$$

To study the properties of the $N \neq 0$ Landau level, we stop the renormalization at $L = \Delta/\epsilon_N$ when the running cutoff reaches the observation energy. The new parameters are

$$\tilde{\alpha} = \frac{\alpha}{Z^2}, \quad \tilde{\epsilon} = \frac{\epsilon}{Z}, \quad Z = \sqrt{1 - 2\alpha \ln \frac{\Delta}{\epsilon_N}}. \tag{A14}$$

Now, we employ the SCBA equation (A3) with the renormalized parameters. The logarithmic term is absent as long as the running cutoff equals ϵ_N after renormalization. The SCBA equation involves a single Landau level and yields the renormalized self-energy $\tilde{\Sigma}(\tilde{\epsilon})$. In the center of Landau level, the imaginary part of $\tilde{\Sigma}$ is

$$\tilde{\gamma} = \omega_c \sqrt{\tilde{\alpha}}/2. \tag{A15}$$

The energy dependence of $\mathrm{Im}\,\tilde{\Sigma}$ gives the renormalized density of states $\tilde{\rho}(\tilde{\epsilon})$. In order to calculate the observable density of states, we use the identity $\rho/\tilde{\rho} = \partial\tilde{\epsilon}/\partial\epsilon$ and obtain

$$\rho(\epsilon) = \frac{\sqrt{\alpha\omega_c^2 - (\epsilon - \epsilon_N Z)^2}}{2\pi^2 v_0^2 \alpha}. \tag{A16}$$

This result has the same form as the result of SCBA [Eq. (A7)], but the parameters $\gamma = \tilde{\gamma}Z$ and Z are modified.

At the lowest Landau level, we use Eqs. (A8) with renormalized parameters and omitted logarithmic terms. We calculate two self-energies, $\tilde{\Sigma}_{1,2}$; their imaginary parts at $\epsilon = 0$ are

$$\tilde{\gamma}_1 = 0, \quad \tilde{\gamma}_2 = \omega_c \sqrt{\tilde{\alpha}/2}. \tag{A17}$$

The renormalized density of states is concentrated in sublattice B,

$$\tilde{\rho}_1 = 0, \quad \tilde{\rho}_2 = \frac{\sqrt{2\tilde{\alpha}\omega_c^2 - \tilde{\epsilon}^2}}{4\pi^2 v_0^2 \tilde{\alpha}}. \tag{A18}$$

In order to find the observable densities, we have to modify our RG scheme. Different values of $\tilde{\rho}_{1,2}$ call for introducing the two different energies, $\epsilon_{1,2}$, in two sublattices. The equations for these energies have the form

$$\frac{d\epsilon_1}{d\log L} = \alpha\epsilon_2, \quad \frac{d\epsilon_2}{d\log L} = \alpha\epsilon_1. \tag{A19}$$

The solution reads

$$\tilde{\epsilon}_{1,2} = \frac{1}{2}[\epsilon_{1,2}(Z + Z^{-1}) + \epsilon_{2,1}(Z - Z^{-1})]. \tag{A20}$$

The connection between ρ and $\tilde{\rho}$ has the form

$$\rho_\nu = \sum_{\mu=1,2} \frac{\partial\tilde{\epsilon}_\mu}{\partial\epsilon_\nu}\tilde{\rho}_\mu. \tag{A21}$$

By using Eqs. (A18), (A20), and (A21), we obtain the resulting density of states at the lowest Landau level in two sublattices,

$$\begin{Bmatrix} \rho_1 \\ \rho_2 \end{Bmatrix} = \begin{Bmatrix} \alpha\ln(\Delta/\omega_c) \\ 1 - \alpha\ln(\Delta/\omega_c) \end{Bmatrix} \frac{\sqrt{2\alpha\omega_c^2 - \epsilon^2}}{4\pi^2 v_0^2 \alpha}. \tag{A22}$$

This result is also similar to its SCBA counterpart [Eq. (A11)] with slightly modified parameters. The width of the Landau level is $\gamma = \tilde{\gamma}_2 Z$. The lowest Landau level becomes isolated when ω_c exceeds $\Delta e^{-1/2\alpha}$.

We can further improve the result by employing the exact density of states at the lowest Landau level found by Wegner.[60] After eliminating all nonzero Landau levels with the help of RG, we find ourselves in the situation when the approach of Ref. 60 is directly applicable and yields

$$\tilde{\rho}_2 = \frac{F(\tilde{\epsilon}/\tilde{\gamma}_2)}{2\pi^2 l_B^2 \tilde{\gamma}_2}, \quad F(x) = \frac{(2/\sqrt{\pi})e^{x^2}}{1 + \left[(2/\sqrt{\pi})\int_0^x e^{y^2}dy\right]^2}. \tag{A23}$$

By substituting this result into Eq. (A21), we calculate the observable density of states,

$$\begin{Bmatrix} \rho_1 \\ \rho_2 \end{Bmatrix} = \begin{Bmatrix} \alpha\ln(\Delta/\omega_c) \\ 1 - \alpha\ln(\Delta/\omega_c) \end{Bmatrix} \frac{F(\epsilon/\gamma)}{2\pi^2 l_B^2 \gamma}. \tag{A24}$$

This improves the result (A22) by replacing the semicircle function $F(x) = \sqrt{1 - x^2/4}$ with the exact lowest Landau level shape, Eq. (A23).

APPENDIX B: DERIVATION OF THE SIGMA MODEL

1. Sigma model in a single valley

Nonlinear sigma model is an effective low-energy theory describing soft modes of the system: diffusons and Cooperons.[36] In the absence of valley mixing, the sigma model for graphene in zero magnetic field was derived in Ref. 27. Here, we generalize this derivation, allowing for the magnetic field within a single valley. Then, we will also include the intervalley scattering.

We start the derivation from the fermionic action (A12). The RA structure of the fields will play a crucial role in the sigma model. Our calculation is based on the SCBA approach outlined above. The more rigorous RG calculation can also be used (as in the zero-B case[23]) as a basis for the sigma model, leading to the same form of the theory.

The $(\bar{\psi}\psi)^2$ term in Eq. (A12) is decoupled with the help of an auxiliary 8×8 supermatrix field R. Subsequent Gaussian integration over ψ yields an effective action in terms of R,

$$S[R] = \frac{\mathrm{Str}\, R^2}{4\pi v_0^2 \alpha} + \mathrm{Str}\ \ln[\epsilon - H - R]. \tag{B1}$$

The soft modes of the system that sigma model deals with describe the fluctuation near the saddle point of $S[R]$. This saddle point is determined by the self-consistency equations (A2) with the self-energy Σ replaced by the matrix R. We separate the real and imaginary parts of the self-energy,

$$R = \mathrm{Re}\,\Sigma + i\tilde{\Gamma}\Lambda, \tag{B2}$$

where $\tilde{\Gamma}$ is the matrix of renormalized scattering rates, $\tilde{\Gamma}=\mathrm{diag}\{\tilde{\gamma}_1,\tilde{\gamma}_2\}_{AB}$, given by Eq. (A6) or (A10). A whole saddle manifold can be generated from the solution (B2) by a uniform rotation T that commute with the Hamiltonian H. As a result, the matrix Λ in the imaginary part of Eq. (B2) replaces with $Q=T^{-1}\Lambda T$. The 4×4 matrix Q operates in RA and BF spaces and obeys the constraints $\mathrm{str}\, Q=0$ and $Q^2=1$. We rewrite the action (B1) in terms of Q omitting the first term that produces an unphysical constant,

$$S[Q] = \mathrm{Str}\ \ln[\tilde{\epsilon} - H + i\tilde{\Gamma}Q], \tag{B3}$$

The real part of the self-energy is included in $\tilde{\epsilon}$, which becomes an AB matrix. Effective low-energy action (sigma model) is a result of the gradient expansion of Eq. (B3). This expansion is a nontrivial procedure in view of the topology of the saddle manifold.[25] Furthermore, the Dirac nature of electrons in graphene gives rise to extra anomalous contributions to the sigma-model action.[27]

The approach of Ref. 27 is directly applicable to the derivation of the sigma model in the magnetic field. The key feature of this approach is a special form of boundary conditions involving the mass term, $m\sigma_3$, in the Hamiltonian. We assume that the mass is zero in the bulk of the sample and gradually increases up to some large value M near the boundary.

We first consider the real part of the action (B3). It is conveniently represented in the form

$$S_1[Q] = \frac{1}{2}\mathrm{Str}\ \ln[\tilde{\epsilon} - H + i\tilde{\Gamma}Q]\tilde{\Gamma}^{-1}[\tilde{\epsilon} - H - i\tilde{\Gamma}Q]$$

$$= \frac{1}{2}\mathrm{Str}\ \ln[G_+^{-1}\tilde{\Gamma}^{-1}G_-^{-1} + \mathbf{j}\,\nabla\, Q]. \tag{B4}$$

Here, we define the matrix Green functions as $G_\pm^{-1}=\tilde{\epsilon}-m\sigma_z + i\boldsymbol{\sigma}\nabla \pm i\tilde{\Gamma}\Lambda$ and current operator $\mathbf{j}=v_0\boldsymbol{\sigma}$. The matrices $G_\pm$ are diagonal in RA space with retarded and advanced Green functions as their elements, $G_+=\mathrm{diag}\{G^R,G^A\}$ and $G_-=\mathrm{diag}\{G^A,G^R\}$. By expanding Eq. (B4) to the second order in ∇Q and using the identity $G^R-G^A=-2iG_-\tilde{\Gamma}G_+$, we get the gradient term of the sigma-model action,

$$S_1[Q] = -\frac{g_{xx}}{8}\mathrm{Str}(\nabla Q)^2. \tag{B5}$$

The factor g_{xx} in this equation is the dimensionless (in units e^2/h) longitudinal conductivity given by the standard Kubo formula,

$$g_{xx} = -\frac{1}{2}\mathrm{Tr}[j_x(G^R - G^A)j_x(G^R - G^A)]. \tag{B6}$$

The calculation of the imaginary part $iS_2[Q]$ is more subtle. We use the representation $Q=T^{-1}\Lambda T$ and cycle the matrices under the supertrace. The resulting expression depends on the vector $\mathbf{u}=T\nabla T^{-1}$,

$$iS_2[Q] = \frac{1}{2}\mathrm{Str}[\ln(G_+^{-1} + i\mathbf{ju}) - \ln(G_-^{-1} + i\mathbf{ju})].$$

The permutation of matrices leading to this formula is equivalent to a rotation of fermion fields, $\psi\mapsto T\psi$, in Eq. (A12). This is not an innocent procedure in view of quantum anomaly.[61] However, such anomalous contributions from the two logarithms cancel in $iS_2[Q]$. We proceed with expanding $iS_2[Q]$ in powers of $\mathbf{u}$. The first two terms of this expansion are

$$iS_2^{(1)} = \pi\,\mathrm{Str}(\Lambda\mathbf{Ju}), \tag{B7}$$

$$iS_2^{(2)} = \frac{g_{xy}^I\epsilon_{\alpha\beta}}{2}\mathrm{Str}(u_\alpha\Lambda u_\beta) = \frac{g_{xy}^I}{4}\mathrm{Str}(Q\nabla_x Q\nabla_y Q). \tag{B8}$$

The factors in Eqs. (B7) and (B8) are the current spectral density $\mathbf{J}(\mathbf{r})$ and the classical part of Hall conductivity,[25]

$$\mathbf{J} = \frac{i}{2\pi}\mathrm{Tr}[\mathbf{j}(G^R - G^A)], \tag{B9}$$

$$g_{xy}^I = \frac{1}{2}\mathrm{Tr}[j_x(G^R - G^A)j_y(G^R + G^A)]. \tag{B10}$$

The net current, and hence the linear term (B7), is absent in the bulk of the system. It is incorrect, however, to drop this term. The contribution $iS_2^{(1)}$ accounts for the edge current and gives the quantum part of the Hall conductivity. We use the infinite mass boundary conditions assuming that $m(\mathbf{r})$ changes from zero inside the sample to another large value M outside it. The gradient of mass is not vanishing near the edge only. We further assume that the mass variation is slow on the scale of the electron mean free path but fast compared to sigma-model length scales. This allows us to perform an expansion of the Green functions in Eq. (B9) in ∇m. With the help of identity $[\mathbf{r},G]=iG\mathbf{j}G$, we obtain

$$J_\alpha(\mathbf{r}) = -\frac{\nabla_\beta m}{2\pi}\mathrm{tr}[j_\alpha G^R \sigma_z G^R j_\beta G^R - j_\alpha G^A \sigma_z G^A j_\beta G^A]_{\mathbf{r},\mathbf{r}}$$
$$= \epsilon_{\alpha\beta}\frac{\partial g_{xy}^{II}}{\partial m}\nabla_\beta m. \quad \text{(B11)}$$

The emerged trace is a mass derivative of the quantum part, g_{xy}^{II}, of the Hall conductivity,[25]

$$g_{xy}^{II} = \frac{ie}{2}\mathrm{Tr}[(xj_y - yj_x)(G^R - G^A)]. \quad \text{(B12)}$$

Substituting Eq. (B11) into Eq. (B7) and integrating over the boundary strip, we express the term (B7) as an integral along the edge and then apply the Stokes theorem,

$$iS_2^{(1)} = \frac{1}{4}[g_{xy}^{II}(0) - g_{xy}^{II}(M)]\mathrm{Str}(Q\nabla_x Q\nabla_y Q). \quad \text{(B13)}$$

To derive the last expression, we have used the identity $\epsilon_{\alpha\beta}\nabla_\alpha u_\beta = \epsilon_{\alpha\beta}u_\beta u_\alpha$.

Collecting all the contributions, we get the final sigma-model action for the single-valley Dirac fermions in the magnetic field,

$$S[Q] = \frac{1}{4}\mathrm{Str}\left[-\frac{g_{xx}}{2}(\nabla Q)^2 + \frac{\theta}{2\pi}Q\nabla_x Q\nabla_y Q\right], \quad \text{(B14)}$$

with the topological angle

$$\theta = 2\pi[g_{xy}^I(0) + g_{xy}^{II}(0) - g_{xy}^{II}(M)]. \quad \text{(B15)}$$

The parameters of the model are determined by the standard Kubo expressions [Eqs. (B6), (B10), and (B12)]. Trace in Eq. (B12) is divergent and requires a regularization. This happens because g_{xy}^{II} accounts for the contribution of edge modes to Hall conductivity. That is why we had to specify boundary conditions in order to find g_{xy}^{II}.

The dependence of g_{xy}^{II} on boundary conditions shows that the very notion of the single-valley Hall conductivity cannot be properly defined. The observable Hall conductivity,

$$g_{xy} = g_{xy}^I + \frac{1}{2}(g_{xy}^{II} - g_{xy}^{II}|_{B\to -B}), \quad \text{(B16)}$$

always includes contributions from both mutually time-reversed valleys implying a cancellation of divergences in Eq. (B12). Considering the Hall conductivity per valley, one usually means a half of the total observable Hall conductivity. This corresponds to a certain regularization requiring $g_{xy}^{II}=0$ at the Dirac point.

At the same time, the value of θ in the sigma-model action is well defined (modulus 2π) even within a single valley as long as θ contains a difference of two g_{xy}^{II} quantities [Eq. (B15)]. At the boundary, the introduced mass M is large, so we can neglect energy and magnetic field there and obtain $g_{xy}^{II}(0) - g_{xy}^{II}(M) = (1/2)\mathrm{sgn}\, M$. This provides the anomalous topological term in the sigma model [Eq. (3)] with $\theta = g_{xy} + (1/2)\mathrm{sgn}\, M$. The sign of the anomalous term ($\mathrm{sgn}\, M$ here) is immaterial as it only changes the action by an integer multiple of $2\pi i$.

It is worth emphasizing that the localization or criticality is the property of the bulk theory and does not depend on the boundary condition. Nevertheless, similarly to the ordinary QHE, introducing the boundary turns out to be a convenient way of deriving the field theory since the action contains a topological term. The resulting theory, however, does not depend on whether a system with boundary or without it (say, on a sphere) is considered and on the way the boundary is implemented. Indeed, the final form of the topological term in Eq. (3) is represented as a 2D integral over the bulk. Thus, the boundary only facilitates revealing and exploring the intrinsic topological properties of Dirac fermions in the bulk of graphene.

An alternative derivation of the sigma model for Dirac fermions employs non-Abelian bosonization[29] that does not require an introduction of boundary conditions. In bosonic language, disorder leads to constraint on the boson field reducing the chiral gauge symmetry group down to sigma-model manifold. The Wess–Zumino term in the bosonized action transforms into the anomalous topological term of the sigma model. This method was used in Ref. 24 for graphene with mixed valleys.

2. Intervalley scattering

Let us now add an intervalley scattering term to the fermionic action (A12). The intervalley scattering due to time-reversal invariant disorder is described by two coupling constants, $\beta_\perp$ and β_z (see Ref. 26 for details),

$$S_{\mathrm{mix}} = 2\pi v_0^2\,\mathrm{Str}\{\beta_\perp[(\psi\bar{\psi})_{AK}(\psi\bar{\psi})_{AK'} + (\psi\bar{\psi})_{BK}(\psi\bar{\psi})_{BK'}]$$
$$+ \beta_z[(\psi\bar{\psi})_{AK}(\psi\bar{\psi})_{BK'} + (\psi\bar{\psi})_{BK}(\psi\bar{\psi})_{AK'}]\}. \quad \text{(B17)}$$

We will perturbatively treat this term within the SCBA scheme. This is equivalent to replacing a pair of ψ fields with the corresponding Green function which, on the saddle-point level, is equal to the matrix Q,

$$(\psi\bar{\psi})_{K,K'} \mapsto \frac{\tilde{\Gamma}_{K,K'}Q_{K,K'}}{2\pi v_0^2\alpha}. \quad \text{(B18)}$$

The imaginary part of self-energy is different in two valleys, $\tilde{\Gamma}_K = \mathrm{diag}\{\tilde{\gamma}_1, \tilde{\gamma}_2\}_{AB}$, $\tilde{\Gamma}_{K'} = \mathrm{diag}\{\tilde{\gamma}_2, \tilde{\gamma}_1\}_{AB}$. After the substitution (B18), the valley-mixing action acquires the form of Eq. (5). We calculate the mean free time from the width of Landau level, $\tau = 1/(4\gamma)$, and obtain in the level's center,

$$\frac{\tau_{\mathrm{mix}}}{\tau} = \frac{2\omega_c\alpha^2}{2\pi\beta_\perp\tilde{\gamma}_1\tilde{\gamma}_2 + \pi\beta_z(\tilde{\gamma}_1^2 + \tilde{\gamma}_2^2)}. \quad \text{(B19)}$$

The form of the S_{mix} term is universal and does not rely on the particular disorder model. At the same time, the mixing rate τ_{mix} is determined by microscopic nonuniversal mechanisms and depends on the disorder type. A potential disorder provides only the intervalley coupling $\beta_\perp$. By using the SCBA results [Eqs. (A6) and (A10)], we find

$$\frac{\tau_{\mathrm{mix}}}{\tau}=\begin{cases}\dfrac{4\alpha[1-\alpha\ln(\Delta/\epsilon_N)]}{\pi\beta_\perp}, & N\neq 0\\ \dfrac{2[1-\alpha^2\ln^2(\Delta/\omega_c)]}{\pi\beta_\perp\ln(\Delta/\omega_c)}, & N=0.\end{cases} \tag{B20}$$

In order to apply the ballistic RG approach, we first renormalize the action (A12) including the mixing term (A17). Assuming the inequality $\alpha \gg \beta_{\perp,z}$, we employ the simplified version of RG equations,[23,26]

$$\frac{d\beta_\perp}{d\ln L}=4\alpha\beta_z, \quad \frac{d\beta_z}{d\ln L}=-2\alpha\beta_z+2\alpha\beta_\perp, \tag{B21}$$

in addition to Eq. (A13). The renormalized couplings are then substituted into Eq. (B19) with the parameters $\tilde{\gamma}_{1,2}$ given by Eqs. (A15) and (A17). In terms of bare couplings α and $\beta_\perp$ (potential disorder), the mixing time is

$$\frac{\tau_{\mathrm{mix}}}{\tau}=\begin{cases}\dfrac{4\alpha}{\pi\beta_\perp}, & N\neq 0\\ \dfrac{2}{\pi\beta_\perp\ln\dfrac{\Delta}{\omega_c}\left[1-2\alpha\ln\dfrac{\Delta}{\omega_c}+\dfrac{4\alpha^2}{3}\ln^2\dfrac{\Delta}{\omega_c}\right]}, & N=0.\end{cases} \tag{B22}$$

For the lowest Landau level, the RG rate $\tilde{\gamma}_1$ appears to be zero[32] since the wave function solely resides in sublattice B. The valley mixing occurs only due to β_z disorder. For potential impurities, this coupling has been absent in the ultraviolet limit but is generated by the RG flow [Eq. (B21)].

The SCBA and RG results [Eqs. (B20) and (B22)] coincide up to a numerical factor of order unity once the Landau levels are well separated, i.e., in the range of our interest. The criterion of level separation is provided by RG calculation: $\omega_c > \Delta e^{-1/2\alpha}$.

*Also at A.F. Ioffe Physico-Technical Institute, 194021 St. Petersburg, Russia.

†Also at Petersburg Nuclear Physics Institute, 188300 St. Petersburg, Russia.

[1] K. S. Novoselov, A. K. Geim, S. V. Morozov, D. Jiang, Y. Zhang, S. V. Dubonos, I. V. Grigorieva, and A. A. Firsov, Science **306**, 666 (2004).

[2] A. K. Geim and K. S. Novoselov, Nat. Mater. **6**, 183 (2007).

[3] A. H. Castro Neto, F. Guinea, N. M. R. Peres, K. S. Novoselov, and A. K. Geim, arXiv:0709.1163, Rev. Mod. Phys. (to be published).

[4] K. S. Novoselov, A. K. Geim, S. V. Morozov, D. Jiang, M. I. Katsnelson, I. V. Grigorieva, S. V. Dubonos, and A. A. Firsov, Nature (London) **438**, 197 (2005); K. S. Novoselov, E. McCann, S. V. Morozov, V. I. Falko, M. I. Katsnelson, U. Zeitler, D. Jiang, F. Schedin, and A. K. Geim, Nat. Phys. **2**, 177 (2006).

[5] Y. Zhang, Y.-W. Tan, H. L. Stormer, and P. Kim, Nature (London) **438**, 201 (2005); Y. Zhang, Z. Jiang, J. P. Small, M. S. Purewal, Y.-W. Tan, M. Fazlollahi, J. D. Chudow, J. A. Jaszczak, H. L. Stormer, and P. Kim, Phys. Rev. Lett. **96**, 136806 (2006).

[6] Z. Jiang, Y. Zhang, H. L. Stormer, and P. Kim, Phys. Rev. Lett. **99**, 106802 (2007).

[7] K. S. Novoselov, Z. Jiang, Y. Zhang, S. V. Morozov, H. L. Stormer, U. Zeitler, J. C. Maan, G. S. Boebinger, P. Kim, and A. K. Geim, Science **315**, 1379 (2007).

[8] D. A. Abanin, K. S. Novoselov, U. Zeitler, P. A. Lee, A. K. Geim, and L. S. Levitov, Phys. Rev. Lett. **98**, 196806 (2007).

[9] K. v. Klitzing, G. Dorda, and M. Pepper, Phys. Rev. Lett. **45**, 494 (1980).

[10] *The Quantum Hall Effect*, edited by R. E. Prange and S. M. Girvin (Springer, New York, 1987).

[11] V. P. Gusynin and S. G. Sharapov, Phys. Rev. Lett. **95**, 146801 (2005).

[12] Y. Zheng and T. Ando, Phys. Rev. B **65**, 245420 (2002).

[13] N. M. R. Peres, F. Guinea, and A. H. Castro Neto, Phys. Rev. B **73**, 125411 (2006).

[14] T. Ando, A. B. Fowler, and F. Stern, Rev. Mod. Phys. **54**, 437 (1982).

[15] D. E. Khmel'nitskii, Helv. Phys. Acta **65**, 164 (1992).

[16] A. W. W. Ludwig, M. P. A. Fisher, R. Shankar, and G. Grinstein, Phys. Rev. B **50**, 7526 (1994).

[17] F. D. M. Haldane, Phys. Rev. Lett. **61**, 2015 (1988).

[18] D. E. Khmelnitskii, Phys. Lett. **106A**, 182 (1984).

[19] R. B. Laughlin, Phys. Rev. B **23**, R5632 (1981).

[20] B. I. Halperin, Phys. Rev. B **25**, 2185 (1982).

[21] B. Huckestein, Rev. Mod. Phys. **67**, 357 (1995).

[22] F. Evers and A. D. Mirlin, arXiv:0707.4378, Rev. Mod. Phys. (to be published).

[23] I. L. Aleiner and K. B. Efetov, Phys. Rev. Lett. **97**, 236801 (2006).

[24] A. Altland, Phys. Rev. Lett. **97**, 236802 (2006).

[25] A. M. M. Pruisken, Nucl. Phys. B **235**, 277 (1984); *The Quantum Hall Effect* (Ref. 10), p. 117.

[26] P. M. Ostrovsky, I. V. Gornyi, and A. D. Mirlin, Phys. Rev. B **74**, 235443 (2006).

[27] P. M. Ostrovsky, I. V. Gornyi, and A. D. Mirlin, Phys. Rev. Lett. **98**, 256801 (2007).

[28] A. A. Nersesyan, A. M. Tsvelik, and F. Wenger, Phys. Rev. Lett. **72**, 2628 (1994); Nucl. Phys. B **438**, 561 (1995); A. M. Tsvelik, Phys. Rev. B **51**, 9449 (1995).

[29] M. Bocquet, D. Serban, and M. R. Zirnbauer, Nucl. Phys. B **578**, 628 (2000); A. Altland, B. D. Simons, and M. R. Zirnbauer, Phys. Rep. **359**, 283 (2002).

[30] I. F. Herbut, Phys. Rev. B **75**, 165411 (2007).

[31] E. V. Gorbar, V. P. Gusynin, and V. A. Miransky, arXiv:0710.3527 (unpublished).

[32] M. Koshino and T. Ando, Phys. Rev. B **75**, 033412 (2007).

[33] D. N. Sheng, L. Sheng, and Z. Y. Weng, Phys. Rev. B **73**, 233406 (2006).

[34] P. Goswami, X. Jia, and S. Chakravarty, Phys. Rev. B **76**, 205408 (2007).

[35] E. McCann, K. Kechedzhi, V. I. Fal'ko, H. Suzuura, T. Ando, and B. L. Altshuler, Phys. Rev. Lett. **97**, 146805 (2006).

[36] K. B. Efetov, *Supersymmetry in Disorder and Chaos* (Cam-

bridge University Press, Cambridge, 1996).
[37] S. Ryu, C. Mudry, H. Obuse, and A. Furusaki, Phys. Rev. Lett. **99**, 116601 (2007).
[38] D. E. Khmelnitskii, JETP Lett. **38**, 552 (1984).
[39] Y. Huo, R. E. Hetzel, and R. N. Bhatt, Phys. Rev. Lett. **70**, 481 (1993); B. M. Gammel and W. Brenig, *ibid.* **73**, 3286 (1994); Z. Wang, B. Jovanović, and D.-H. Lee, *ibid.* **77**, 4426 (1996); S. Cho and M. P. A. Fisher, Phys. Rev. B **55**, 1637 (1997); L. Schweitzer and P. Markoš, Phys. Rev. Lett. **95**, 256805 (2005).
[40] Z. Wang, M. P. A. Fisher, S. M. Girvin, and J. T. Chalker, Phys. Rev. B **61**, 8326 (2000).
[41] A. M. M. Pruisken and I. S. Burmistrov, Ann. Phys. (N.Y.) **316**, 285 (2005).
[42] L. W. Engel, D. Shahar, C. Kurdak, and D. C. Tsui, Phys. Rev. Lett. **71**, 2638 (1993).
[43] D. K. K. Lee and J. T. Chalker, Phys. Rev. Lett. **72**, 1510 (1994).
[44] K. Nomura and A. H. MacDonald, Phys. Rev. Lett. **96**, 256602 (2006).
[45] L. Sheng, D. N. Sheng, F. D. M. Haldane, and L. Balents, Phys. Rev. Lett. **99**, 196802 (2007).
[46] K. Yang, S. Das Sarma, and A. H. MacDonald, Phys. Rev. B **74**, 075423 (2006).
[47] P. M. Ostrovsky, I. V. Gornyi, and A. D. Mirlin, Eur. Phys. J. Spec. Top. **148**, 63 (2007).
[48] F. V. Tikhonenko, D. W. Horsell, R. V. Gorbachev, and A. K. Savchenko, Phys. Rev. Lett. **100**, 056802 (2008).
[49] T. Ando, J. Phys. Soc. Jpn. **75**, 074716 (2006).
[50] Y.-W. Tan, Y. Zhang, H. L. Stormer, and P. Kim, Eur. Phys. J. Spec. Top. **148**, 15 (2007).
[51] M. I. Katsnelson and A. K. Geim, Philos. Trans. R. Soc. London, Ser. A **366**, 195 (2008).
[52] D. V. Khveshchenko, Phys. Rev. B **75**, 241406(R) (2007).
[53] S. Hikami, M. Shirai, and F. Wegner, Nucl. Phys. B **408**, 415 (1993).
[54] Y. Aharonov and A. Casher, Phys. Rev. A **19**, 2461 (1979).
[55] M. F. Atiyah and I. M. Singer, Ann. Math. **87**, 485 (1968); **87**, 546 (1968); **93**, 119 (1971); **98**, 139 (1971).
[56] J.-S. Caux, Phys. Rev. Lett. **81**, 4196 (1998).
[57] A. J. M. Giesbers, U. Zeitler, M. I. Katsnelson, L. A. Ponomarenko, T. M. G. Mohiuddin, and J. C. Maan, Phys. Rev. Lett. **99**, 206803 (2007).
[58] E. McCann and V. I. Fal'ko, Phys. Rev. Lett. **96**, 086805 (2006).
[59] N. H. Shon and T. Ando, J. Phys. Soc. Jpn. **67**, 2421 (1998).
[60] F. Wegner, Z. Phys. B: Condens. Matter **51**, 279 (1983); E. Brezin, D. J. Gross, and C. Itzykson, Nucl. Phys. B **235**, 24 (1984).
[61] K. Fujikawa, Phys. Rev. D **21**, 2848 (1980).